

## **Seafloor cratering and sediment remolding at sites of fluid escape**

Matt O'Regan<sup>1</sup>, Matthias Fortwick<sup>2</sup>, Martin Jakobsson<sup>1</sup>, Kathryn Moran<sup>3</sup>, David Mosher<sup>4</sup>

### **Supplementary Information**

#### **Consolidation characteristics of modeled sediments**

Consolidation parameters for the three soil types used in the model were derived from a synthesis of consolidation test results. These were performed on fine-grained terrigenous sediments collected from the Equatorial Atlantic (Demerara Rise), Gulf of Mexico (Ursa Basin) and the Arctic Ocean (Lomonosov Ridge). The key parameters extracted from the tests were the void ratio upon deposition (at 1 kPa) ( $e_o$ ), the Compression Index ( $C_c$ ), and the Recompression Index ( $C_r$ ). A linear relationship exists between  $e_o$  and  $C_c$  (Fig DR1), defining a broad compressibility range for these sediments. Using this relationship, 3 idealized sediments were selected with a high, average and low  $C_c$  (Table 1, Fig. DR1). The  $C_r$  was calculated using the linear regression between  $C_c$  and  $C_r$  from the measured samples (Fig. DR1).

The incremental load consolidation tests from ODP Leg 207, Site 1261, Demerara Rise, were published by O'Regan and Moran (2007). Long et al. (2008) published results from constant rate of strain consolidation tests from IODP Leg 308, Sites 1322 and 1324, Ursa Basin, Gulf of Mexico. Although  $e_o$  was not reported for these tests, the processed data were downloaded and used to calculate both  $C_c$  and  $e_o$  (Table DR1). Data from the Lomonosov Ridge are compiled from published results of IODP expedition 302 (O'Regan et al., 2010), and 6 new tests performed on samples collected during the LOMROG III expedition in 2012, and the 2014 SWERUS-C3 expedition, both conducted from the Swedish icebreaker *Oden*. Core names and sample depths for all the tests are provided in Table DR1. Results from the unpublished tests are shown in Fig. DR2.

#### **Remolding influence on $C_c$**

To further verify the influence of remolding on the  $C_c$ , a comparison was made between the consolidation tests performed on intact samples from the LOMROG-III

and SWERUS-C3 expeditions, and tests where the trimmings from the intact sample were remolded prior to consolidation (Fig. DR3). Remolding was performed by placing the trimmings from the intact test inside an airtight bag and manually reworking the sediments for a period of 5 minutes.

### **Example calculation of settlement from remolding**

A 1 m tall layer of sediment, buried at a depth of 100 mbsf, is initially under hydrostatic pore pressure conditions. The average bulk density of the overlying material is  $1.8 \text{ g/cm}^3$ .

The initial vertical effective stress ( $\sigma'_v$ ) is calculated by;

$$\sigma'_v = (\rho_B - \rho_W)gz - u_e$$

$$\sigma'_v = (1.8 \text{ g/cm}^3 - 1.024 \text{ g/cm}^3)9.81 \text{ ms}^{-2} \cdot 100 \text{ m} - 0$$

$$\sigma'_v = 761 \text{ kPa}$$

Assuming engineering properties for the sediments so that  $C_c=0.55$ ,  $e_o=2.56$ , and  $C_r=0.118$  (Table 1), the in-situ void ratio is calculated from,

$$e_{insitu} = e_o - C_c \text{Log}(\sigma'_v)$$

$$e_{insitu} = 2.56 - 0.55 \cdot \text{Log}(761 \text{ kPa})$$

$$e_{insitu} = 0.971$$

giving a fractional porosity of 0.493.

When the pore pressure increases to equal the initial effective vertical stress (761 kPa) the sediments may rebound (or expand in volume). This unloaded void ratio would be;

$$e_{rebound} = e_{insitu} + C_r \text{Log} \left( \frac{\sigma'_{v1}}{\sigma'_{v2}} \right)$$

$$e_{rebound} = 0.971 + 0.118 \cdot \log\left(\frac{761 \text{ kPa}}{761 \text{ kPa}}\right)$$

$$e_{rebound} = 1.311$$

giving a fractional porosity of 0.567.

The change in height of the 1 m tall sediment layer can be calculated from the change in void ratio during unloading,

$$\Delta h = \frac{(e_{final} - e_{initial})}{(1 + e_{initial})} \cdot H_{initial}$$

$$\Delta h = \frac{(1.311 - 0.971)}{(1 + 0.971)} \cdot 1 \text{ m}$$

$$\Delta h = 0.173 \text{ m}$$

So that the unloaded height of the layer is

$$H_{unloaded} = H_{initial} + \Delta h = 1.17 \text{ m}$$

If the sediments do not expand volumetrically during the decrease in effective stress, the void ratio during unloading remains constant (0.971), and the height of the layer remains 1 m.

To mimic the widespread failure and mobilization of sediments, we assume that fluidization and remolding occurs when effective stresses equal 1 kPa. Remolding changes the compression index ( $C_c$ ) of the sediments to the intrinsic compression index ( $C_c^*$ ).  $C_c^*$  is predicted based upon the in-situ void ratio when the sediments are remolded ( $e_L$ ) using the equation provided by Burland (1990);

$$Cc^* = 0.256 \cdot e_L - 0.04$$

In the case where the void ratio has rebounded during unloading, this results in,

$$Cc^* = 0.256 \cdot (1.311) - 0.04$$

$$Cc^* = 0.30$$

and if no rebound occurs during unloading,

$$Cc^* = 0.256 \cdot (0.971) - 0.04$$

$$Cc^* = 0.21$$

As overpressure is dissipated, the vertical effective stress increases until it again reaches 761 kPa. During this time the sediments consolidate along the intrinsic compression line, so that,

$$e_{final} = e_{unloaded} + C_c^* \text{Log} \left( \frac{\sigma'_{V1}}{\sigma'_{V2}} \right)$$

For the 2 cases above, the final void ratio is found by,

a) with rebound during unloading

$$e_{final} = 1.311 + 0.3 \cdot \text{Log} \left( \frac{1 \text{ kPa}}{761 \text{ kPa}} \right)$$

$$e_{final} = 0.447$$

giving a fractional porosity of 0.309.

The change in height of the remolded and reconsolidated section is,

$$\Delta h = \frac{(0.447 - 1.311)}{(1 + 1.311)} \cdot 1.17 \text{ m}$$

$$\Delta h = -0.437$$

and the new height of the layer,

$$H_{remolded} = H_{initial} + \Delta h = 1.17 \text{ m} - 0.44 \text{ m} = 0.73 \text{ m}$$

This represents a 27% reduction in the height of the original 1 m sediment layer.

b) With no rebound during unloading,

$$e_{final} = 0.971 - 0.21 \cdot \log\left(\frac{1 \text{ kPa}}{761 \text{ kPa}}\right)$$

$$e_{final} = 0.366$$

giving a fractional porosity of 0.268.

The change in height is,

$$\Delta h = \frac{(0.366 - 0.971)}{(1 + 0.971)} \cdot 1.0 \text{ m}$$

$$\Delta h = -0.307$$

and the new remolded height of the layer,

$$H_{remolded} = H_{initial} + \Delta h = 1.0 \text{ m} - 0.31 \text{ m} = 0.69 \text{ m}$$

This represents a 31% reduction in the height of the original 1 m sediment layer.

## Table Captions

**Table DR1.** Sample list and test type for data shown in Fig. DR1 and DR2. Test types are: INCL=incremental load; CRS=constant rate of strain.

**Table DR2.** Sample list and test type for data shown in Fig. DR1 and DR2. Test types are: INCL=incremental load; CRS=constant rate of strain.

## Figure Captions

**Fig. DR1.**  $C_c$  versus  $e_o$  for consolidation samples from Demerara Rise, Ursa Basin, and the Lomonosov Ridge. Three representative idealized soils were defined to capture the range in compressibility for these sediments. Inset illustrates the relationship between  $C_c$  and  $C_r$ . The regression was used to calculate  $C_r$  for the idealized sediments.

**Fig. DR2.** Incremental load consolidation results from 6 samples collected from the Lomonosov Ridge on the LOMROG-III and SWERUS-C3 expeditions.

**Fig. DR3.** Intact versus remolded incremental load consolidation results from LOMROG-III and SWERUS-C3 samples. In all cases the remolded compression index ( $C_c^*$ ) is lower than the intact sample (Table DR1), implying a lower void ratio for the remolded samples at comparative effective stresses. In all but one sample this trend persists to effective stresses  $>10000$  kPa. In one sample, the void ratios converge when the effective stress  $>10000$  kPa.

## References

- Long, H., Flemings, P.B., Germaine, J.T., Saffer, D.M., and Dugan, B., 2008. Data report: consolidation characteristics of sediments from IODP Expedition 308, Ursa Basin, Gulf of Mexico. In Flemings, P.B., Behrmann, J.H., John, C.M., and the Expedition 308 Scientists, *Proc. IODP*, 308: College Station, TX (Integrated Ocean Drilling Program Management International, Inc.). doi:10.2204/iodp.proc.308.204.2008
- O'Regan, M., Moran, K., Baxter, C. D. P., Cartwright, J., Vogt, C., Kölling, M., (2010). Towards ground truthing exploration in the central Arctic Ocean: a Cenozoic compaction history from the Lomonosov Ridge. *Basin Research*, 22, 215-235. doi:10.1111/j.1365-2117.2009.00403.x
- O'Regan, M., and Moran, K. (2007). Compressibility, permeability, and stress history of sediments from Demerara Rise. In Mosher, D.C., Erbacher, J., and Malone, M.J. (Eds.), *Proc. ODP, Sci. Results*, 207: College Station, TX (Ocean Drilling Program), 1–35. doi:10.2973/odp.proc.sr.207.114.2007

## Tables and Figures

Table DR1.

Sample	Depth (mbsf)	Test Type	$C_c$	$E_o$	$C_r$
SWERUS-C3-30-GC-2-138-145	2.27	INCL	0.634	2.764	0.109
SWERUS-C3-29PC-3-140-145	3.77	INCL	0.471	2.180	0.088
SWERUS-C3-29PC-3-145-150	3.82	INCL	0.342	1.606	0.049
LOMROG12-PC10-1-100-106	0.90	INCL	0.311	1.637	0.052
LOMROG12-PC10-3-142-148	3.90	INCL	0.362	1.852	0.068
LOMROG12-PC10-5-135-140	6.81	INCL	0.383	1.890	0.088
IODP-302-3A-3H-3, 125-130	18.62	INCL	0.433	1.990	0.107
IODP-302-3A-3H-3, 130-135	18.67	INCL	0.405	1.883	0.107
IODP-302-2A-10X-1, 141-146	42.97	INCL	0.375	1.764	0.095
IODP-302-2A-10X-1, 146-151	43.02	INCL	0.341	1.639	0.086
IODP-302-2A-20X-1, 141-146	87.61	INCL	0.355	1.785	0.086
IODP-302-2A-20X-1, 146-151	87.66	INCL	0.353	1.764	0.104
IODP-302-2A-38X-5, 0-5	171.11	INCL	0.509	2.452	0.123
IODP-302-2A-38X-5, 5-10	171.16	INCL	0.491	2.376	0.133
ODP-207-1261A-4R-2-90A	72.00	INCL	0.670	2.940	0.120
ODP-207-1261A-4R-2-90B	72.00	INCL	0.830	3.540	0.180
ODP-207-1261A-6R-6-134	198.00	INCL	0.800	3.540	0.180
ODP-207-1261A-9R-5-139	264.00	INCL	0.760	3.420	0.170
ODP-207-1261A-13R-4-140	301.00	INCL	0.580	2.780	0.120
IODP-308-U1324C-6H-3WR	304.02	CRS	0.304	1.634	0.042
IODP-308-U1324C-6H-3WR	303.94	CRS	0.269	1.520	0.044

IODP-308-U1324C-1H-01WR	51.21	CRS	0.413	2.062	0.037
IODP-308-U1324C-1H-01WR	51.14	CRS	0.439	2.244	0.067
IODP-308-U1324B-13H-7WR	117.40	CRS	0.361	1.881	0.073
IODP-308-U1324B-4H-7WR	32.14	CRS	0.531	2.505	0.127
IODP-308-U1324B-4H-7WR	32.10	CRS	0.436	2.033	0.112
IODP-308-U1324B-7H-7WR	60.62	CRS	0.350	1.787	0.086
IODP-308-U1324B-26H-3WR	220.34	CRS	0.288	1.714	0.075
IODP-308-U1324B-31H-3WR	261.02	CRS	0.250	1.494	0.061
IODP-308-U1324B-21H-3WR	183.14	CRS	0.318	1.741	0.078
IODP-308-U1322D-3H-3WR	103.44	CRS	0.275	1.561	0.073
IODP-308-U1322D-2H-02WR	72.78	CRS	0.468	2.241	0.111
IODP-308-U1324C-1H-01WR	51.27	CRS	0.489	2.420	0.114
IODP-308-U1324B-4H-07WR	31.86	CRS	0.385	1.962	0.072
IODP-308-U1324B-15H-05WR	134.20	CRS	0.252	1.482	0.052
IODP-308-U1322B-15H-01WR	126.28	CRS	0.312	1.743	0.050
IODP-308-U1322B-18H-06WR	157.42	CRS	0.285	1.672	0.036
IODP-308-U1324B-23H-05WR	200.00	CRS	0.272	1.541	0.047
IODP-308-U1324B-10H-07WR	89.22	CRS	0.318	1.779	0.073
IODP-308-U1322B-4H-03WR	27.21	CRS	0.505	2.514	N/A
IODP-308-U1322D-1H-02WR	42.87	CRS	0.455	2.235	0.104

Table DR2.

INTACT SAMPLE	Cc	Eo	Cr
SWERUS-C3-30-GC-2-138-145	0.634	2.764	0.109
SWERUS-C3-29PC-3-140-145	0.471	2.180	0.088
SWERUS-C3-29PC-3-145-150	0.342	1.606	0.049
LOMROG12-PC10-1-100-106	0.311	1.637	0.052
LOMROG12-PC10-3-142-148	0.362	1.852	0.068
LOMROG12-PC10-5-135-140	0.391	1.925	0.088
REMOLDED SAMPLE			
SWERUS-C3-29PC-3-140-145-R	0.363	1.602	0.083
LOMROG12-PC10-1-100-106-R	0.270	1.303	0.061
LOMROG12-PC10-3-142-148-R	0.304	1.555	0.074
LOMROG12-PC10-5-135-140-R	0.279	1.494	0.086

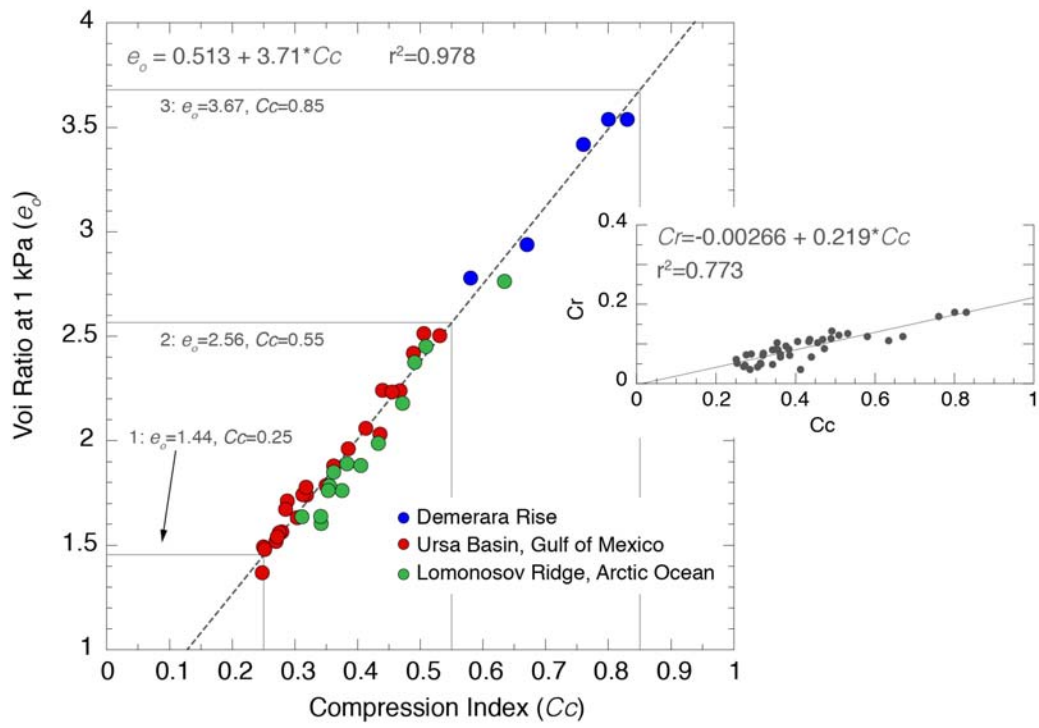


Fig DR1.

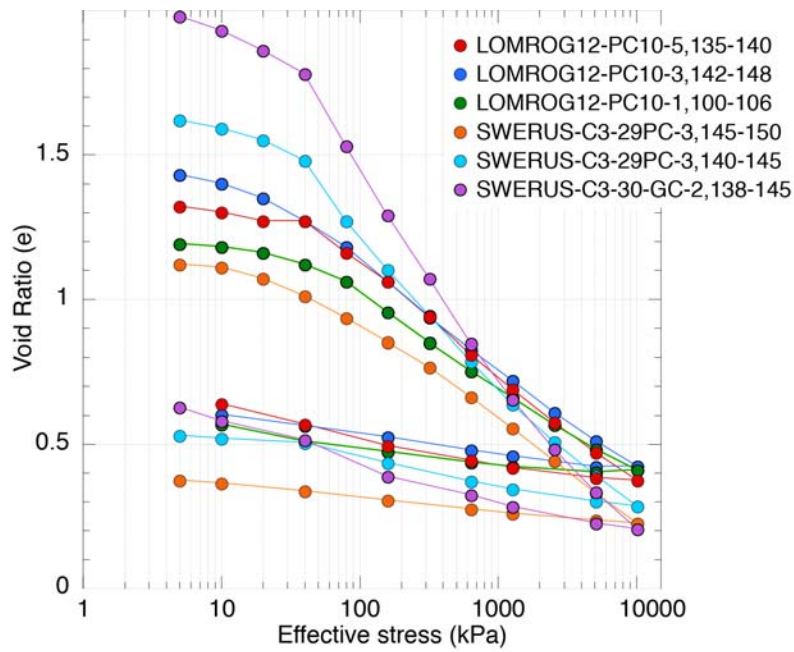


Fig. DR2.



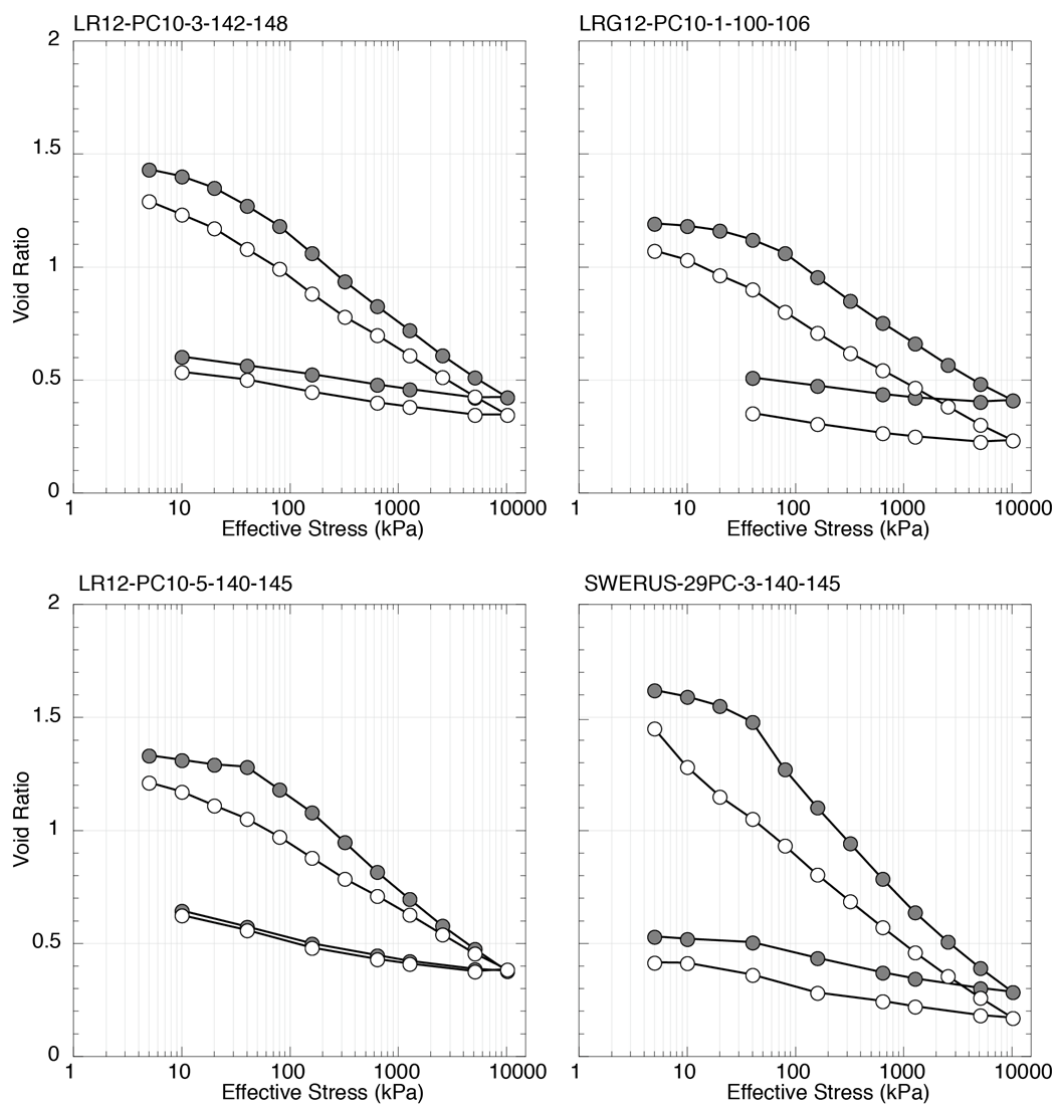


Fig. DR3.